

A High-Efficiency X-band Microwave Power Amplifier for AESA Radar System

Pham Cao Dai

Institute of System Integration
Le Quy Don Technical University
236 Hoang Quoc Viet, HN, Vietnam
Email: daipc.isi@lqdtu.edu.vn

Le Dai Phong

Institute of System Integration
Le Quy Don Technical University
236 Hoang Quoc Viet, HN, Vietnam
Email: phongld@mta.edu.vn

Luu Van Tuan

Institute of System Integration
Le Quy Don Technical University
236 Hoang Quoc Viet, HN, Vietnam
Email: tuanlv.isi@lqdtu.edu.vn

Luong Duy Manh

Faculty of Radio-Electronic Engineering
Le Quy Don Technical University
236 Hoang Quoc Viet, HN, Vietnam
Email: duymanhcs2@mta.edu.vn

Dao Thanh Toan

Vietnam-Japan R&D Center
University of Transport and Communications, Hanoi, Vietnam
3 Cau Giay, HN, Vietnam
Email: daotoan@utc.edu.vn

Abstract—This paper proposes a high-efficiency microwave power amplifier operating at X-band using an adaptive bias method for AESA radar application. The designed power amplifier delivers 5 W at 9.5 GHz with more than 40% of PAE and 10 dB Gain. The designed power amplifier was designed in a Keysight ADS software. To meet requirements of the AESA radar system, an adaptive bias technique is employed to prevent degradation of the PA performance with respect to the variation of the input power. The simulated results show that by making a proper adjustment of drain bias voltage from 22 V to 32 V, performance of the PA can be remained regardless of input power change from 22 dBm to 30 dBm.

I. INTRODUCTION

Recently, X-band active electronically scanned array (AESA) radar system [1][2] has been receiving significant considerations due to its promising advantages. An illustration of such a AESA system is indicated in Fig. 2. An array of antennas combination with an array of transmitter(TX)/Receiver(RX) module forms a beam of radio waves which can be directed to different directions without physically moving the antennae. Each TX/RX module consists of a power amplifier (PA) and other individual components. One of the most important requirements for the AESA system is how to reduce power consumption of the system. This is because the number of transmitter(TX)/Receiver(RX) module used is large creating high power consumption. This issue becomes more serious when operation frequency increases. In such a system, PA plays a key role since it consumes mostly energy of the system. This means PA used in the AESA system needs to operate efficiently with high-efficiency (high power added efficiency - PAE) and high gain in a wide input power range while still ensuring sufficient output power. In this paper, a high efficient PA has been designed to meet these stringent requirements of

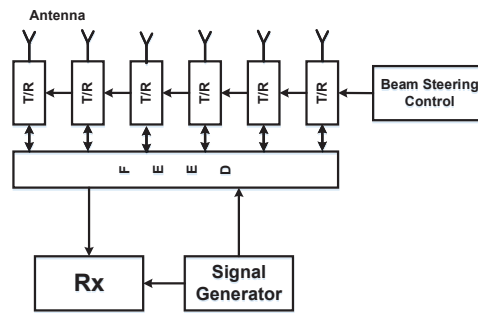


Fig. 1. Illustration of an AESA system.

the AESA system. In order to have high efficiency a harmonic termination approach [3][4] is employed to suppress dissipated power in harmonics. Because second harmonic plays a critical role for PAE improvement [5], in the design phase second harmonic termination is carefully realized. Moreover, to ensure high gain and high efficiency in a wide input power range, an adaptive bias technique is used. This method is realized by adjusting the drain bias voltage of the designed PA whenever input power varies from low to high regions. This helps the PA to remain high efficiency, gain and output power regardless of the input power change.

II. POWER AMPLIFIER DESIGN

The schematic of the PA is shown in Fig. 3. Input matching network (IMN) and output matching network (OMN) use open-ended stubs to realize short-circuited for second harmonic ($2f_0$) and third harmonic ($3f_0$) minimizing power dissipation at these harmonics. The matching networks are realized using microstrip lines on a RO4350B substrate with a thickness of 10 mil. Dimensions of the microstrip lines of the IMN and

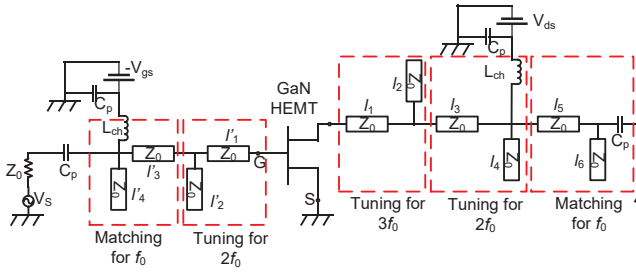


Fig. 2. Schematic of the designed PA.

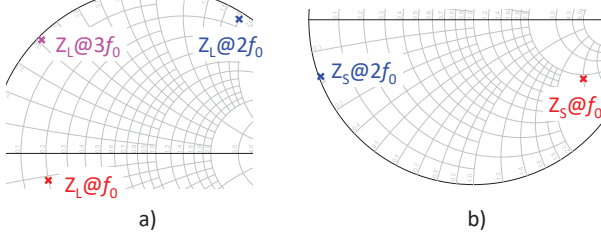


Fig. 3. Optimum source and load impedances represented on the Smith chart.

OMN are as given follows: $w = 0.8$ mm, $l_1 = 3.08$ mm, $l_2 = 1.0$ mm, $l_3 = 0.49$ mm, $l_4 = 2.36$ mm, $l_5 = 0.25$ mm, $l_6 = 5.45$ mm, $l'_1 = 4.4$ mm, $l'_2 = 1.5$ mm, $l'_3 = 0.91$ mm, $l'_4 = 3.92$ mm. In the figure, $C_p = 1.1$ pF is a RF-bypass capacitor while L_{ch} functions as a RF choke. In final layout this inductor is replaced by a quarter wavelength transmission line. A GaN HEMT TGF2977-SM small-signal and large-signal model are provided by Qorvo [6]. The large-signal model of the GaN HEMT is constructed from a non-linear Angelov model. Lumped components models are provided by Murata. Figure 3 shows realized optimum load and source impedances at fundamental ($f_0 = 9.5$ GHz) and $2f_0 = 19$ GHz, $3f_0 = 28.5$ GHz by the IMN and OMN. The optimum impedances initially are found by using a load/source pull technique in Keysight ADS [7]. Here, it is noted that the IMN is designed to treat up to second harmonic while up to third harmonic is treated by the OMN. It can be seen in the figure that the second and third harmonic impedances are located at the boundary of the Smith chart indicating a purely reactive impedances. This helps to minimize the harmonics power. Insertion losses at 9.5 GHz of the designed IMN and OMN are 0.5 dB and 0.43 dB, respectively. These losses are relatively low at X-band frequency. The transistor is biased in a class-AB operation with $V_{ds} = 32$ V and $V_{gs} = -2.8$ V for a drain current of 25 mA.

A. Small-signal evaluation

Figure 4 shows return losses of the designed PA including input and output return losses. The return loss response shown in Fig. 4 indicates a low return

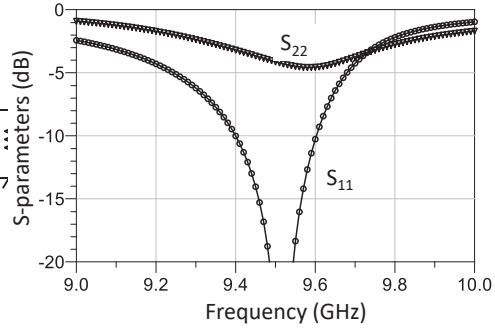


Fig. 4. Simulated return losses of the designed PA.

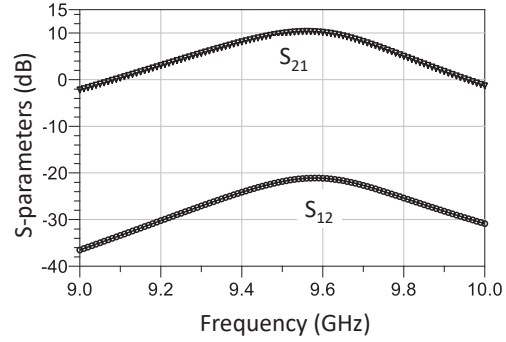


Fig. 5. Simulated gain and isolation of the designed PA.

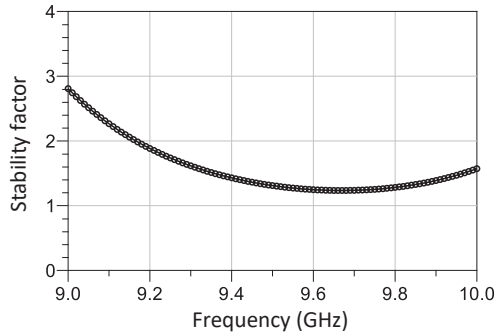


Fig. 6. Stability response of the designed PA.

loss in the frequency range from 9 GHz to 10 GHz. Figure 5 indicates the simulated results for small-signal power gain (S_{21}) and reversed isolation (S_{12}) of the designed. The figure shows a high gain of 11 dB at around 9.5 GHz and low isolation of -20 dB at this frequency point.

To avoid unintentional spurious oscillation for the designed PA, the stability has to be greater than unity. This is indicated in Fig. 6 where simulated stability factor of the PA is given. It can be seen that from 9.0 GHz to 10.0 GHz the designed PA is stable.

B. Large-signal evaluation

Finally, large-signal performance of the designed PA is evaluated in simulation with variation of drain bias

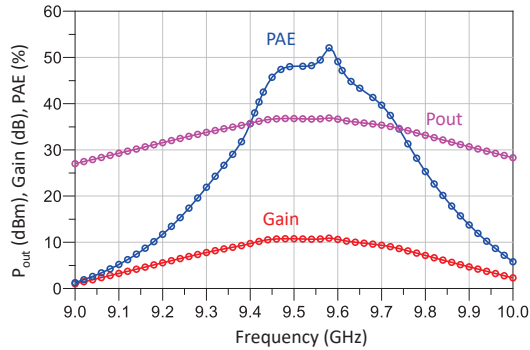


Fig. 7. Frequency response of large-signal performance of the designed PA.

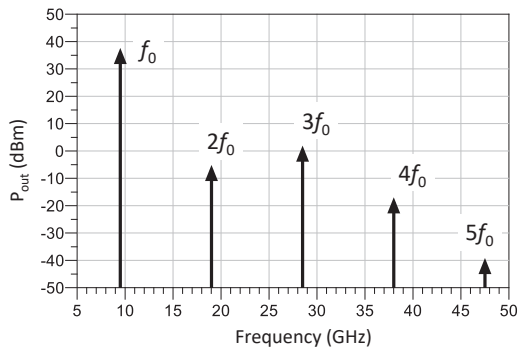


Fig. 8. Output spectrum of the designed PA.

voltage V_{ds} . The drain bias voltage is varied to check optimum performance while changing input power. The large-signal performance is evaluated by using a Harmonic Balance analysis in ADS. Figure 7 shows the simulated results of PAE, Gain and output power (Pout) as a function of operation frequency from 9 GHz to 10 GHz. As can be seen in the figure, PAE can remain above 40% while the Gain can remain more than 10 dB from 9.4 GHz to 9.7 GHz. This means the performance of the designed PA can remain in a 300 MHz bandwidth validating the design method. Figure 8 shows output spectrum of the designed PA to verify the second harmonic termination. As can be seen in the figure, the second harmonic is significantly attenuated by 42 dB compared with the fundamental tone. To meet necessary requirements for AESA system which means the designed PA needs to still remain performance during variation of input power. This can be feasible by using an adaptive control of the drain bias voltage (V_{ds}). The method is indicated in Fig. 9. The figure shows the dependence of PAE and Pout as a function of Pin with changing V_{ds} . In this investigation, V_{ds} varies from 22 V to 32 V while V_{gs} remains a constant value of -2.8 V. As can be seen in the figure, at low power range from 22 dBm to 25 dBm, output power is almost constant while PAE changes significantly with

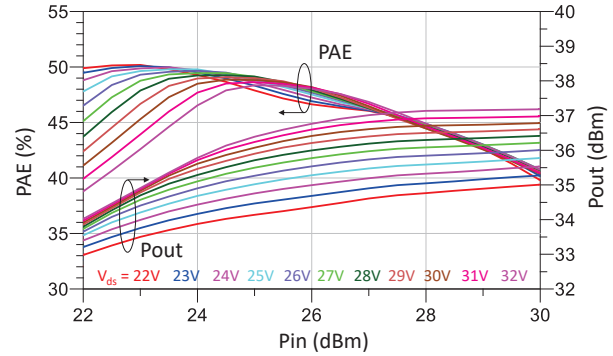


Fig. 9. Large-signal performance as a function of input power with varying V_{ds} .

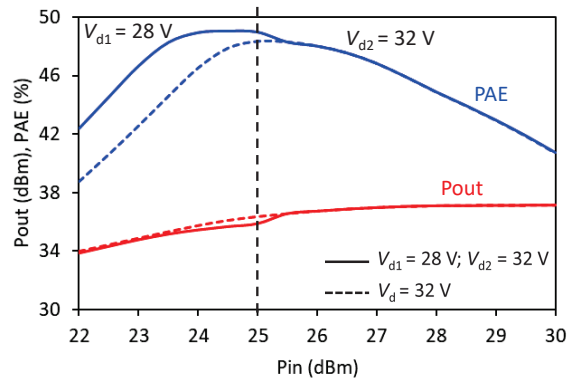


Fig. 10. Control of V_{ds} to remain the PA's performance.

$V_{ds} = 26$ V - 32 V. The lower the V_{ds} , the higher PAE. This means by lowering V_{ds} output power can almost remain constant while PAE can be improved. This is because DC power consumption is reduced when V_{ds} decreases. On the other hand, in the higher power range from 25 dBm to 30 dBm, PAE is almost constant whereas output power changes remarkably with changing V_{ds} . In this region, V_{ds} should be at high values to keep sufficient output power without degradation of PAE. This trend can be further understood by looking at Fig. 10 which shows an example of adjusting V_{ds} to remain PAE and output power when input power varies. As can be clearly seen in the figure, in the lower power range V_{ds} is set to 28 V to keep high PAE without output power degradation while at high power range V_{ds} is set to 32 V to keep both high PAE and output power. In contrast, if V_{ds} is kept constant at 32 V during input power range from 22 dBm to 30 dBm, PAE drops about 4 % at low power range compared with that of using adjusted V_{ds} .

III. CONCLUSION

This paper presents an adaptive bias method to improve performance of an X-band microwave power amplifier. The PA is first aimed at designing to operate at X-band with a good performance at both small-signal

and large-signal levels. In the small-signal evaluation the designed PA delivers good gain and input/output return losses. In the large-signal evaluation, it offers good PAE, gain and output power. After the design phase, optimum performance for using in the AESA system can be found by varying the drain bias voltage. It has been found that by lowering V_{ds} at the low power range, output power can almost remain constant while PAE can be improved. In the high power range, however, V_{ds} should be high to remain sufficient PAE and output power. The proposed method, thus, helps to keep performance of the designed PA regardless of the input power change.

ACKNOWLEDGMENT

This research is funded by Vietnam National Foundation for Science and Technology Development (NAFOSTED) under grant number 102.04-2018.14.

REFERENCES

- [1] H. Hommel, and H.-P. Feldle, "Current status of airborne active phased array (AESA) radar systems and future trends," *IEEE MTT-S International Microwave Symposium Digest, 2005*, Long Beach, CA, USA, 17 June 2005.
- [2] M. Bulygin, *et al.*, "Digital radar module for digital AESA of spaceborne SAR," *EUSAR 2018, 12th European Conference on Synthetic Aperture Radar*, Aachen, Germany, 4-6 June 2018.
- [3] M. Kamiyama, R. Ishikawa, and K. Honjo, "5.65 GHz high-efficiency GaN HEMT power amplifier with harmonics treatment up to fourth order," *IEEE Microw. Wireless Compon. Lett.*, vol. 22, no. 6, pp. 315 - 317, Jun. 2012.
- [4] T. Yao *et al.*, "Frequency characteristic of power efficiency for 10 W/30 W-class 2 GHz band GaN HEMT amplifiers with harmonic reactive terminations," *Proc. Asia-Pacific Microw. Conf.*, pp. 745-747, Nov. 2013.
- [5] J. Enomoto, R. Ishikawa, and K. Honjo, "Second Harmonic Treatment Technique for Bandwidth Enhancement of GaN HEMT Amplifier With Harmonic Reactive Terminations," *IEEE Trans. Microw. Theory Techn.*, vo. 65, no. 12, pp. 1-6, Dec. 2017.
- [6] URL: <https://www.qorvo.com/>
- [7] URL: <https://www.keysight.com/zz/en/products/software/pathwave-design-software/pathwave-advanced-design-system.html>